Iranian Journal of Materials Forming 11 (3) (2024) 13-20

Online ISSN: 2383-0042

IJMF

Iranian Journal of Materials Forming

Journal Homepage: http://ijmf.shirazu.ac.ir

Research Article

A Study on the Role of Effective Parameters on the Mechanical Properties of Gas Pressure Welded Rebars

B. Ghaffari, H. Daneshmanesh and S.M. Zebarjad*

Department of Materials Science and Engineering, School of Engineering, Shiraz University, Shiraz, Iran

ARTICLE INFO

Article history:

Received 8 June 2024
Reviewed 27 August 2024
Revised 11 September 2024
Accepted 23 September 2024

Keywords:

Gas pressure welding
Rebar diameter
Tensile properties
Microstructure
Bending behavior

Please cite this article as:

Ghaffari, B., Daneshmanesh, H., & Zebarjad, S. M. (2024). A study on the role of effective parameters on the mechanical properties of gas pressure welded rebars. *Iranian Journal of Materials Forming*, *11*(3), 13-20. https://doi.org/10.22099/IJMF.2024.50416.1300

ABSTRACT

Gas pressure welding (GPW) is a type of solid-state welding developed as a branch of the oxyacetylene fuel gas welding process (OFW) that employs mechanical pressure. One of the main advantages of GPW is the reduction of rebar waste, as well as enhancing buildings' earthquake resistance due to the high strength of the rebar connection points. In this research, the factors affecting GPW and the mechanical properties of gas pressure-welded rebars were investigated. Tempcore rebars with diameters of 18 and 25 mm were welded at different pressures (17 to 21 MPa for 18 mm diameter and 22 to 28 MPa for 25 mm diameter) and varying times (40 to 60 seconds for 18 mm diameter and 60 to 110 seconds for 25 mm). Tensile, bending, and microhardness tests were conducted on the samples to evaluate their final properties. Additionally, the microstructure of the samples was examined using both optical and scanning electron microscopes. The results indicate that for Tempcore rebar, increasing pressure and heating time decreases the likelihood of forming oxide layers, resulting in improved ductility of the samples. The tensile test results show that longer heating times provide greater opportunities for recrystallization. The bending test results reveal that reduced pressure and welding time lead to brittleness in the samples, attributed to the presence of oxide particles and delayed recrystallization. Microhardness results show that the highest values are associated with samples welded at low pressure and low welding times.

1. Introduction

Reinforcing bars, commonly referred to as rebars, are used in the building industry to provide tensile strength for concrete structures. Nowadays there are different types of rebar depending on the manufacturing process, such as those produced by the hot rolling process, mechanical heat treatment process (Tempcore), and microalloying additives. Rebars are manufactured according to international standards (such as ASTM A615 and ISO 6935) which specify minimum yield strength, ultimate tensile strength to yield ratio (UTS/YS), elongation at break, carbon content, and carbon equivalent [1]. The yield strength profile plays an important role, particularly in structural stability. In

* Corresponding author
E-mail address: Mojtabazebarjad@shirazu.ac.ir (S. M. Zebarjad)
https://doi.org/10.22099/ijmf.2024.50416.1300

addition, the percentage of carbon and carbon equivalent in steels is used as an index of weldability as well as ductility, and by controlling these elements, different properties of steel can be obtained [2, 3].

The most common method of connecting rebars is the overlapping method, in which the two ends are placed on top of each other and secured by wire. However, this method has many drawbacks. Due to the increase in the volume of the rebars, the concrete does not mix well, and it results in an increase in the overall weight of the structure [4].

According to the AWS D1.1 standard, the connection method that has replaced the overlapping connection is the welding connection. There are various welding methods, with solid-state welding being one option.

In the 1930s, butt welding of reinforcement was developed in the United States of America and Japan as one of the branches of the oxyacetylene gas welding process, known as gas pressure welding (GPW). Since then, this method has been widely used for welding rails and pipes, as well as steel rebars [5]. Rebar gas pressure welding is one of the patching methods employed to reduce the cost of conventional building construction. In this process, the two ends of the rebar are polished and cut at a zero-degree angle by a special cutting machine. Through the heat generated from the combustion of acetylene and oxygen gas, the ends reach the welding temperature (1250 °C), and under hydraulic pressure from the cylinder, they are forged together [6].

One of the main reasons for the development of this method (butt welding of rebar) is the critical need to strengthen and ensure the durability of concrete structures, which results in an increased lifespan and improved financial security for the residents and users of these structures [5].

The most important advantages of the gas pressure welding method include increased joint strength due to the larger diameter of the connection, reduced structural weight by eliminating the covering patch, and improved concrete mixing with rebar due to the reduced volume of the rebar. Despite these advantages, there are some limitations, such as the skill level of the welding operator, the non-implementation or incomplete implementation of PQR (Procedure Qualification Record) and WPS (Welding Procedure Specification) instructions, and the inability to control the heat generated by the oxyacetylene flame [7].

A significant amount of research has been conducted on the gas pressure welding process. For example, Armstrong et al. [8] investigated the effect of oxide particles on mechanical properties. Ryuichi et al. [9] studied the influence of upsetting length and heating time on the morphology of oxide particles in the rail joints. Jeon et al. [10] examined the mechanical properties of gas pressure welded splices of deformed reinforcing bars. Baroutian [11] compared the mechanical properties of overlap welded joints with gas compression joints of rebars. Saito et al. [12] investigated the ultrasonic inspection method for gas pressure connections of rebars and concluded that the results of ultrasonic and tensile tests of the connections are correlated. Issa et al. [13] studied the side-to-side welding connection to determine the appropriate welding length. Moustafa et al. [1] focused on optimizing the butt welding parameters of rebars using the coated electrode method (SMAW). They conducted their research using overlap and butt joint methods. Kheyroddin et al. [14] investigated the behavior of the joint under cyclic loads and its effect on the flexural performance of reinforced concrete joints.

Based on our current understanding, previous research has primarily focused on the key factors affecting gas pressure welding, such as heating time, pressure, cooling speed, and the type of rebar [15-19]. However, these studies have failed to consider the combined impact of adjusting these factors on GPW. With this in mind, our current research aims to investigate the simultaneous influence of pressure and heating time on the properties of welded rebar.

2. Experimental Methods

2.1. Materials

The reinforcing steel bars examined in this study were Tempcore type bars with diameters of 18 and 25, produced according to ASTM A615, grade 60 (yield strength = 420 MPa). Table 1 shows the chemical

composition of the rebar used in the study.

The pressure parameter and heating time for each rebar diameter were varied at three levels. The welded samples were coded as shown in Table 2. D, P, and S represent the diameter of the rebar (18 and 25 mm), the process pressure (17, 19, 20, 21, 24, and 28 MPa), and the heating time (40, 50, 60, 85, and 110 seconds) of the samples, respectively.

Table 1. Chemical composition of the rebars used in this study

C	Mn	Si	Cu	S
0.276	0.801	0.208	0.174	0.0196
Ni	**P**	**Mo**	**Cr**	**Fe**
0.013	0.0365	0.005	0.00037	Balance

Table 2. Welded samples

D18	D18P21S40	D18P19S40	D18P17S40
	D18P21S50	D18P19S50	D18P17S50
	D18P21S60	D18P19S60	D18P17S60
D25	D25P28S60	D25P24S60	D25P20S60
	D25P28S85	D25P24S85	D25P20S85
	D25P28S110	D25P24S110	D25P20S110

2.2. Welding method

In order to perform the GPW process, the following steps were taken:

1. The rebars were cut using a cutter equipped with a WC blade (Fig. 1(a)).
2. The cut rebars were held between two cross heads carefully (Fig. 1(b)).
3. The flame was maintained in a reducing condition by controlling the acetylene/oxygen ratio (Fig. 1(c)). It is worth noting that during flame heating, the rebars are under pressure.
4. Fig. 1(d) shows the final upset welding zone.

2.3. Evaluations

2.3.1. Microscopic evaluation

To clarify the joining conditions of the welded samples, the surfaces of some samples were polished and etched with Nital, and the joints were investigated using an optical microscope (Optika B-383PLi) and a scanning electron microscope (TESCAN Vega 2 LMU). SEM-EDX was also employed to analyze the presence of oxide inclusions and the chemical composition of the base metal near the joint.

2.3.2. Bending test

Since flexural strength plays an important role in the performance of rebars, the current research conducted bending tests according to JIS Z 3881 and JIS Z 2248 standards. The tests were performed at a loading speed of 10 mm/min.

2.3.3. Tensile test

The tensile properties of the welded samples were determined using the tensile test. To do this, the welded samples were tested based on the guidelines proposed in the JIS Z 2241 standard. The cross-head speed for the tensile test was kept constant at 10 mm/min.

2.3.4. Microhardness test

In order to determine the effect of the new parameters on the hardness of welded samples, the Vickers microhardness test was performed according to the ASTM E384 standard, using a diamond pyramid indenter equipped with a 100 gram- weight.

3. Results and Discussion

As previously stated in Table 2, the samples with diameters of 18 and 25 mm were welded at the specified

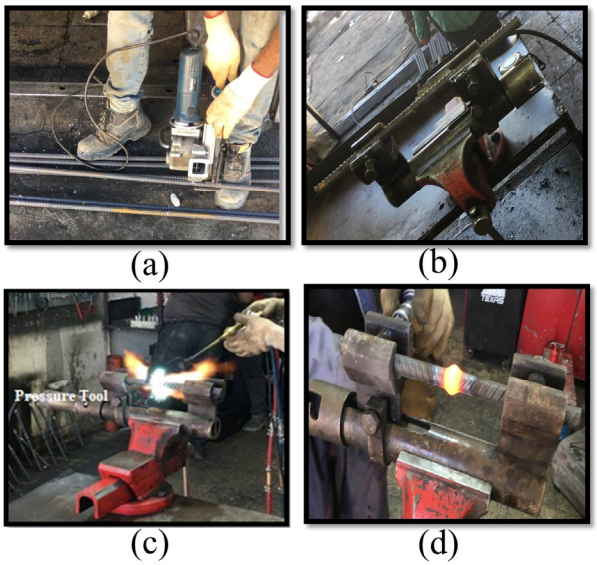

Fig. 1. Welding steps during the GPW process.

heating time and pressure. In this section of the article, the results of the role of GPW parameters on the properties of the welded samples are presented.

3.1. Microstructural study

Fig. 2 shows the optical microscopic image taken from the polished surface of the base metal. The microstructure includes fine pro-eutectoid ferrite and pearlite phases.

Fig. 3(a) and 3(b) show the optical microscopic images taken from the welded zones of the 18 mm and 25 mm rebars, respectively. As can be seen, the microstructure of the rebars depends on both the pressure and the time of welding. Indeed, the microstructure of sample D18P21S60 included ferrite types I and II (Widmanstatten) and fine pearlite. The primary reason for this variation can be attributed to the fact that as welding time increases from 60 to 110 seconds, the ferrites have enough time to nucleate as a type I. This is why there is no evidence of ferrite type II in the D25P28S110 sample.

Fig. 4(a) and 4(b) show the SEM micrographs taken from the polished and etched surfaces of two different rebars (D18P21S60 and D25P28S110) welded under different conditions. As can be seen, the thickness of pearlite layers and their colonies depends on the welding conditions. The thickness of the pearlite layer for rebars for the 18 mm and 25 mm diameters is 460 nm and 223 nm, respectively. The primary reason for this variation can be attributed to the fact that increasing cooling time has an effective role in the nucleation and growth of the pearlite [17].

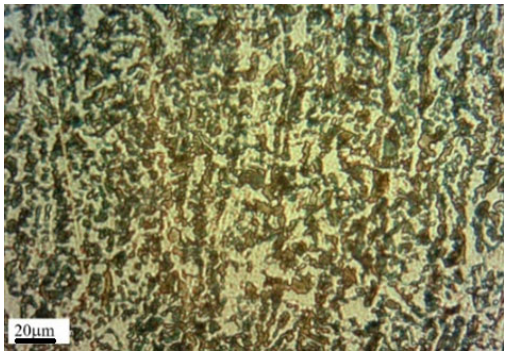

Fig. 2. Microstructure of base metal.

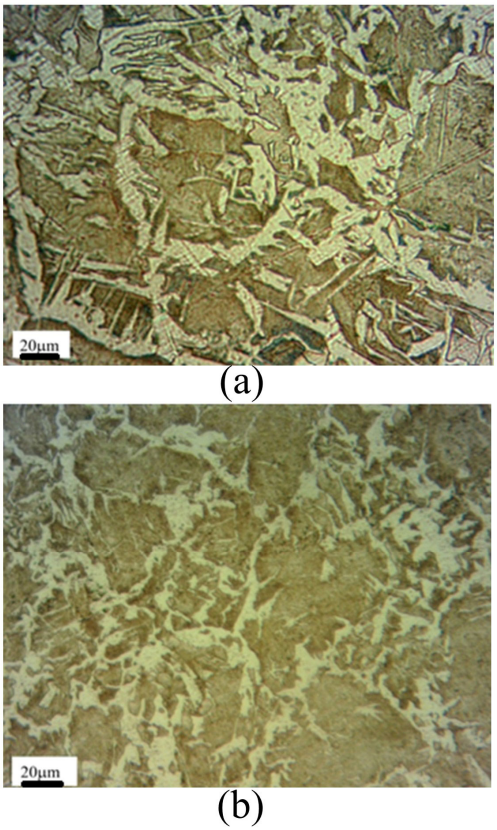

Fig. 3. Optical micrographs of the weld zones for two different samples: (a) D18P21S60 and (b) D25P28S110.

The details of pearlite layers (S_p) and their colony areas (μm^2) for both samples are summarized in Fig. 5. It is worth noting that the colony area was measured using ImageJ software.

In the current research, it was tried to clarify the role of both pressure and welding time on the formation of oxide particles. Fig. 6 shows the dependency of the formation of such oxides on pressure. As can be seen, the oxide particles are located in the welding zone, which is under low pressure and low welding time. This is why, at the beginning of the welding process, the oxide particles can form in the upset of weld. It is clear that the stability of such particles depends strongly on the value of both pressure and welding time. In fact, at high values of both pressure and welding time, those particles gain enough energy to break and decompose; in such cases, the matrix is free of oxides (compare Figs. 6(a) and 6(b)).

According to previous research focused on GPW [6], although the type of flame in the welding zone is a reduction one, there is a possibility of an oxidation process due to the weak protection of the welding

atmosphere or the insufficient acetylene/oxygen ratio. In such cases, oxide layers can form at the interface. There are several ways to prevent the occurrence of oxide particles, such as promoting the reduction behavior of the flame and increasing both pressure and heating time.

The types of oxide particles present in the microstructure of the samples were determined using EDS. These oxide particles are composed of SiO_2 and MnO (Fig. 7).

To investigate the role of pressure on the flow pattern of material during gas pressure welding, the polished surfaces of samples (D25P22S110 and D25P28S110) were over-etched. Fig. 8(a) and 8(b) show the material flow during welding due to the applied pressure. As can be seen, at low pressure, the vortex line is concentrated at the center of the sample, and increasing pressure causes the vortex line to spread toward the welding upset. Fig. 8(c) is a schematic representation that demonstrates how materials flow in the presence of pressure. It is evident that when both high pressure and long duration are present, the material can flow easily from a point outside the welding upset toward it.

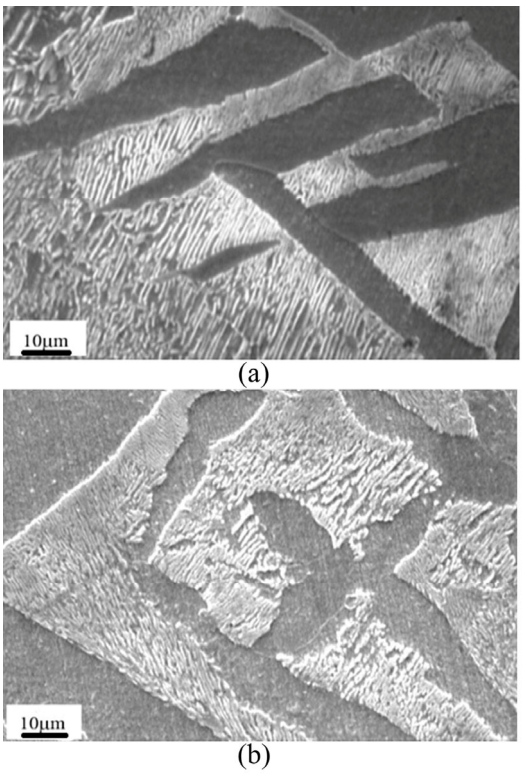

Fig. 4. SEM micrographs of the weld zones for two different samples: (a) D18P21S60 and (b) D25P28S110.

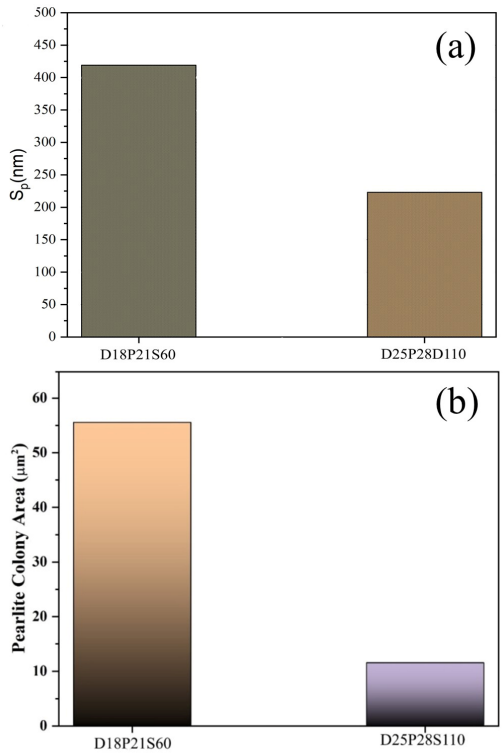

Fig. 5. The dependency of pearlitic specifications on the welding conditions: (a) the thickness of pearlite and (b) the pearlite colony area.

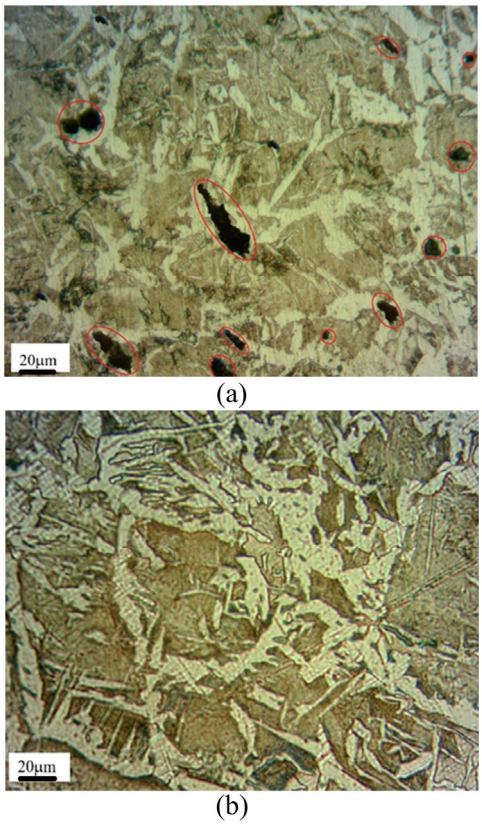

Fig. 6. The presence of oxide particles in the welding zone: (a) D18P17S40 and (b) D18P21S60. The oxide particles are highlighted by a circle.

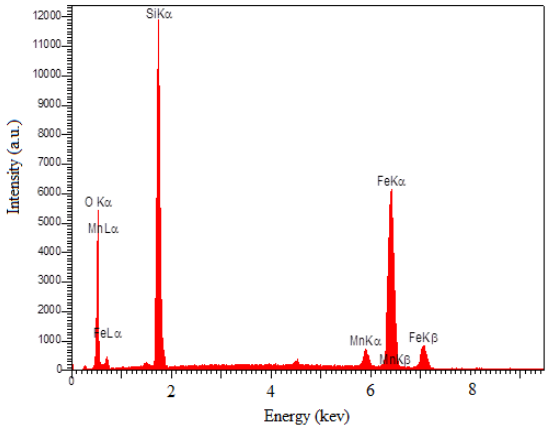

Fig. 7. The result of the EDS.

The pattern of removal of oxide particles from the welding zone to the upset welding zone appears to be similar to that proposed in Fig. 8(c).

3.2. Tensile test

The results of the tensile properties of all welded samples are summarized in Table 3. As seen in Table 3, at a constant diameter (for example, 18 mm), increasing pressure causes a decrease in the strength (both yield and ultimate) of the samples. This is because higher pressure accelerates the conditions for recrystallization (in fact, the crystallization process requires a critical value of deformation; if the magnitude of plastic strain increases, the temperature or time required for recrystallization will decrease). Additionally, as mentioned earlier, the probability of the appearance of oxide particles decreases as pressure increases. Since the samples produced at high pressure are almost free of oxide particles, one may conclude that the matrix lacks strengthening particles, resulting in a decrease in the strength of the steel, unlike its elongation.

3.3. Bending test

According to the JIS Z 3881 standard, the criterion for acceptance is the absence of defects (cracks) in the bending zone after the bending test. Figs. 9(a) and 9(b) show the behavior of two samples during the bending test. As can be seen, the sample welded at high pressure (Fig. 9(a)) bent more than 90° without any visual defects. This implies that these types of samples behave like ductile materials due to the lack of oxide particles and the feasibility of recrystallization resulting from both high pressure and welding time. Fig. 9(b) demonstrates that the sample produced under conditions of low pressure and short welding time exhibited brittleness and ultimately fractured. The main reason for this behavior can be referred to the presence of oxide particles and the delay in the crystallization process [17].

3.4. Microhardness test

Figs. 10(a) and 10(b) show the variation of microhardness along the base metal toward the weld line for various samples. As can be seen, at both low pressure and low welding time, the microhardness is higher than that of the other condition. This is because, under such conditions, the oxide particles do not have enough energy to be removed or decomposed from the weld zone. Additionally, due to the high cooling rate, ferrite type II, which is harder than type I, will be created. Furthermore, the recrystallization process will be postponed due to low plastic deformation and short heating time. The increase in microhardness near the weld zone in all materials is attributed to the presence of oxide particles and the resulting microstructure.

Table 3. Tensile strength of samples under different conditions

Sample code	Ultimate tensile strength (MPa)	Yield stress (MPa)	Elongation (%)
D18P17S40	639	451	12.12
D18P17S50	621	445	12.91
D18P17S60	615	435	13.53
D18P19S40	629	448	12.83
D18P19S50	620	442	13.45
D18P19S60	613	432	13.86
D18P21S40	626	442	12.98
D18P21S50	616	432	13.87
D18P21S60	611	427	14.34
D25P22S60	653	434	19
D25P22S85	651	430	19.5
D25P22S110	648	427	20.5
D25P25S60	646	438	20.5
D25P25S85	641	431	21.3
D25P25S110	633	419	21.6
D25P28S60	655	449	20
D25P28S85	647	428	20.5
D25P28S110	642	424	22

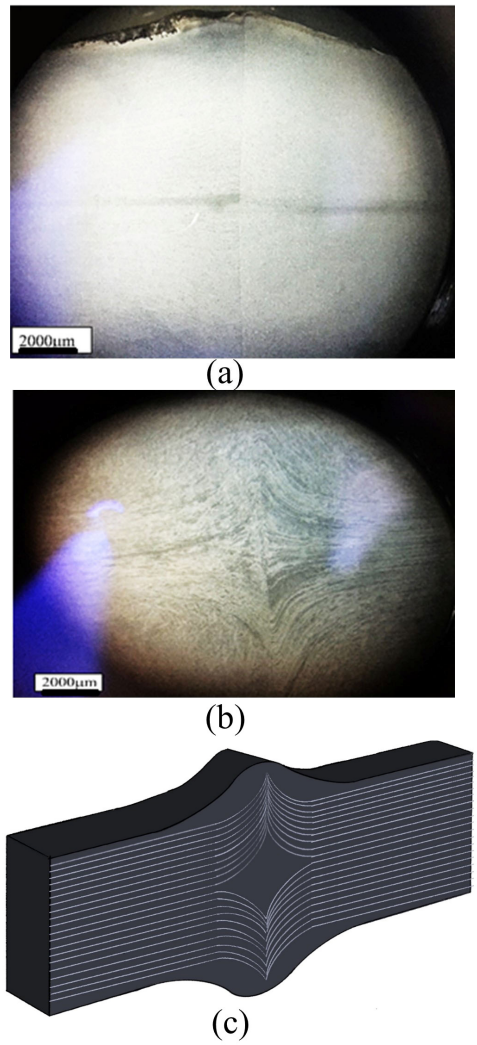

Fig. 8. The effect of pressure and heating time on the flow pattern: (a) D25P22S110, (b) D25P28S110, and (c) schematic of flow pattern.

4. Conclusion

In the current research, two similar rebars with different diameters were welded using the GPW method. The role of different parameters of the GPW method on the mechanical properties of the samples was evaluated. The summary of the results is as follows:

- The final microstructure of samples depends on the pressure and welding time. At both high pressure and welding time, the microstructure includes coarse pearlite and ferrite type I; at both low pressure and short welding time, ferrite type II appears.
- The results of the tensile test show that the highest tensile strength belongs to the samples with 18 and 25 mm diameters welded at both the lowest pressure and shortest times.
- The results of the bending test indicate that the brittle behavior occurs in the samples welded at short welding time.

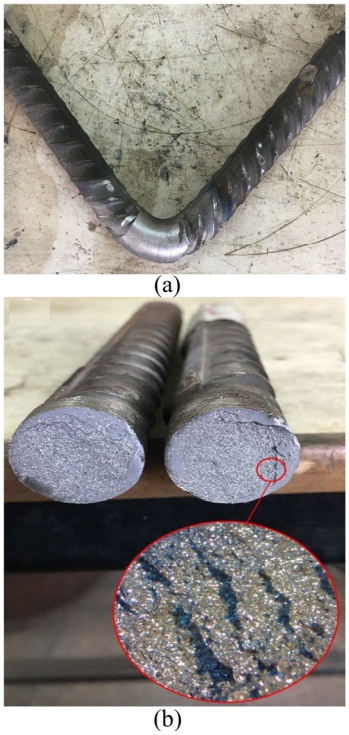

Fig. 9. The bending behavior of welded samples under different conditions: (a) D25P25S110 and (b) D18P17S40.

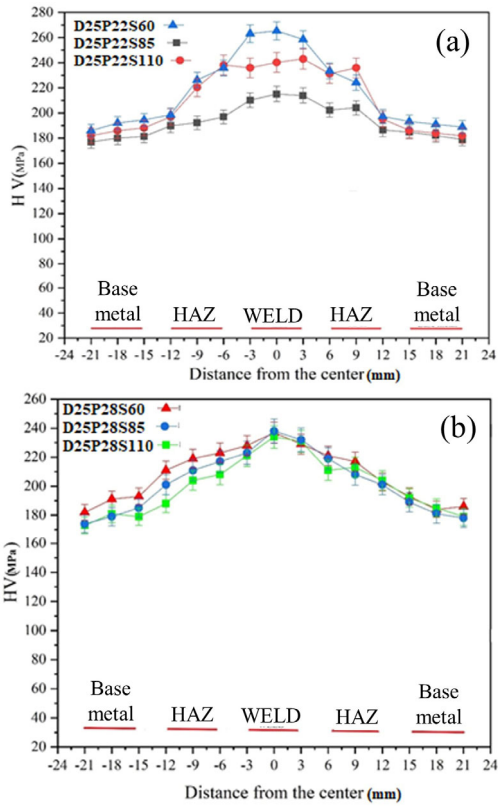

Fig. 10. Profile of microhardness: (a) D25P22S60, D25P22S85 and D25P22S110, (b) D25P28S60, D25P28S85 and D25P28S110.

- The results of the microhardness test show that for all samples, the position of the highest microhardness value is at the weld center.
- The microscopic evaluation shows that with an increase in the diameter of the rebar from 18 to 25 mm, the thickness of the pearlite layers increases from 460 to 223 nm while the colony size in these samples decreases from 56 μm^2 to 13 μm^2, which is attributed to the cooling rate.

Conflict of interest

The authors declare that they have no conflicts of interest.

Funding

This research has not received any funding.

5. References

[1] Moustafa, M. (2016). Optimizing the welding parameters of reinforcing steel bars. *Arabian Journal for Science and Engineering*, *41*(5), 1699-1711. https://doi.org/10.1007/s13369-015-1929-x

[2] Dabiri, H., & Kheyroddin A. (2021). An experimental comparison of RC beam-column joints incorporating different splice methods in the beam. *Structures*, *34*, 1603-1613. https://doi.org/10.1016/j.istruc.2021.08.101

[3] Firmanto, H. (2022) Tensile strength and microstructure of rotary friction welded carbon steel and stainless steel joints. *Journal of Manufacturing and Materials Processing*, *7*(1), 7. https://doi.org/10.3390/jmmp7010007

[4] Zanuy, C., & Díaz I. M. (2018). Stress distribution and resistance of lap splices under fatigue loading. *Engineering Structures*, *175*, 700-710. https://doi.org/10.1016/j.engstruct.2018.08.067

[5] Yamamoto, R. (2007). Advances in gas pressure welding technology for rails. *Railway Technology Avalanche*, *17*, 99-105.

[6] Yamamoto, R., Fukada, Y., Oishibash, H. (1998). Gas pressure welding method for steel reinforcing bars. *Welding Research Supplement*, *77*(5), 188-192.

[7] Alderman, J. (1995). *The January 17, 1995 Kobe earthquake: an EQE summary report*. EQE International, San Francisco.

[8] Armstrong, I. (1971). Full-strength butt welds of reinforcing bars by the pressure-gas process. *Bulletin of the New Zealand Society for Earthquake Engineering, 4*(2), 270-284. https://doi.org/10.5459/bnzsee.4.2.270-284

[9] Ryuichi, Y., Yuichi, K., & Yasuto, F. (2014). Experimental examination for understanding of transition behavior of oxide inclusions on gas pressure weld interface: joining phenomena of gas pressure welding. *Welding International, 28*(7), 510-520. https://doi.org/10.2207/qjjws.28.167

[10] Jeon, J. (2015). A Study on the mechanical properties of gas pressure welded splices of deformed reinforcing bar. *Journal of the Society of Disaster Information*, *11*(4), 520-526. https://doi.org/10.15683/kosdi.2015.11.4.520

[11] Baroutian, M. (2018). *Laboratory investigation of the effect of various factors on the performance of rebar connection by forging method and its comparison with welded connections* [Master's thesis, Shahrood University].

[12] Saito, T., Yabe, Y., & Fujimori, T. (1985). An ultrasonic testing method for gas pressure welded joints of reinforcing steel bars. *Ultrasonics*, *23*(3), 119-127. https://doi.org/10.1016/0041-624X(85)90060-5

[13] Issa, C. A., & Nasr, A. (2006). An experimental study of welded splices of reinforcing bars. *Building and Environment*, *41*(10), 1394-1405. https://doi.org/10.1016/j.buildenv.2005.05.025

[14] Kheyroddin, A., Rouhi, S., & Dabiri, H. (2021). An experimental study on the influence of incorporating lap or forging (GPW) splices on the cyclic performance of RC columns. *Engineering Structures*, *241*, 112434. https://doi.org/10.1016/j.engstruct.2021.112434

[15] Kheyroddin, A., & Dabiri, H. (2020). Cyclic performance of RC beam-column joints with mechanical or forging (GPW) splices; an experimental study. *Structures*, *28*, 2562-2571. https://doi.org/10.1016/j.istruc.2020.10.071

[16] Shokrzadeh, M. R., Nateghi-Alahi, F., Mansoori, M. R., & Javadi, P. (2022). The improvement of the threaded-based mechanical splice by modifying the threaded system: Study of techniques cold rolling and rotating friction welding. *Journal of Building Engineering*, *320*, 126198. https://doi.org/10.1016/j.jobe.2023.107964

[17] Dey, I., Ghosh, S. K., & Saha, R. (2019). Effects of cooling rate and strain rate on phase transformation, microstructure and mechanical behavior of thermomechanically processed pearlitic steel. *Journal of Materials Research and Technology*, *8*(3), 2685-2698. https://doi.org/10.1016/j.jmrt.2019.04.006

[18] Gutscher, D., & Sun, J. (2006). Evaluation of improved gas pressure welding for in-track HAL service. *Railway Track and Structures*, *102*(9).

[19] Sharbatdar, M. K., Jafari, O. M., & Karimi, M. S. (2018). Experimental evaluation of splicing of longitudinal bars with forging welding in flexural reinforced concrete beams. *Advances in Concrete Construction*, *6*(5), 509-525. https://doi.org/10.12989/acc.2018.6.5.509